IISRC International Industrial Scientific Research Corporation
International Conference on Industrial Scientific Research Engineering
www.worldconferences.org

Implementation of IRIS Recognition System using Phase Based Image Matching Algorithm

N. MURALI KRISHNA[1], DR. P. CHANDRA SEKHAR REDDY[2]
[1]Assoc Prof, Dept of ECE, Dhruva Institute of Engineering & Technology, Hyderabad, AP-India,
E-mail: omkrish29@gmail.com.
[2]Prof, Coordinator, Dept of ECE, JNTU, Hyderabad, AP-India, E-mail: drpcsreddy@gmail.com.

Abstract: This paper presents an efficient algorithm for iris recognition using phase-based image matching. The use of phase components in two dimensional discrete Fourier transforms of iris images makes possible to achieve highly robust iris recognition with a simple matching algorithm. Experimental evaluation using the CASIA iris image database(ver. 1.0 and ver. 2.0) clearly demonstrates an efficient performance of the proposed algorithm.

Keywords: CASIA, Iris Images.

I. INTRODUCTION

Biometric authentication has been receiving extensive attention over the past decade with increasing demands in automated personal identification. Among many biometrics techniques, iris recognition is one of the most promising approaches due to its high reliability for personal identification [2–9]. A major approach for iris recognition today is to generate feature vectors corresponding to individual iris images and to perform iris matching based on some distance metrics [4–7]. Most of the commercial iris recognition systems implement a famous algorithm using iris codes proposed by Daugman [4]. One of the difficult problems in feature-based iris recognition is that the matching performance is significantly influenced by many parameters in feature extraction process (eg., spatial position, orientation, center frequencies and size parameters for 2D Gabor filter kernel), which may vary depending on environmental factors of iris image acquisition. Given a set of test iris images, extensive parameter optimization is required to achieve higher recognition rate. Addressing the above problem, as one of the algorithms which compares iris images directly without encoding [8, 9], this paper presents an efficient algorithm using phase-based image matching – an image matching technique using only the phase components in 2D DFTs (Two-Dimensional Discrete Fourier Transforms) of given images. The technique has been successfully applied to high accuracy image registration tasks for computer vision applications [10-12], where estimation of sub-pixel image translation is a major concern. In our previous work [12], on the other hand, we have proposed an efficient fingerprint recognition algorithm using phase-based image matching, and have developed commercial fingerprint verification units. In this paper, we demonstrate that the same technique is also highly effective for iris recognition.

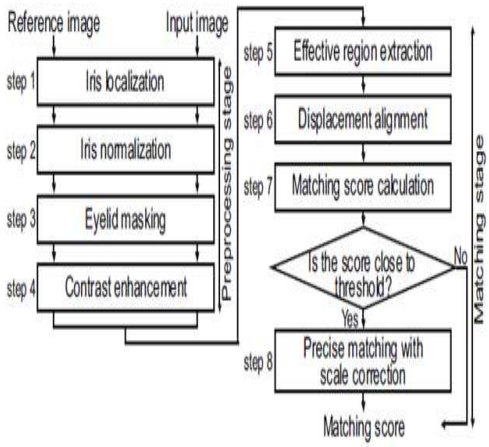

Fig.1. Flow diagram of the proposed algorithm

The use of Fourier phase information of iris images makes possible to achieve highly robust iris recognition in a unified fashion with a simple matching algorithm. Experimental performance evaluation using the CASIA iris image database ver. 1.0 and ver. 2.0 clearly demonstrates an efficient matching performance of the proposed algorithm. Fig.1 shows the overview of the proposed algorithm. The algorithm consists of two stages: (i) preprocessing stage (step 1 – step 4) and (ii) matching stage (step 5 – step 8). Section 2 describes the Phase-Based Iris Recognition Algorithms. Section 3 presents the Iris Recognition System. Section 4 discusses experimental evaluation and finally Section 5 gives the conclusions.

II. PHASE-BASED IRIS RECOGNITION ALGORITHMS

This section describes possible modification of the phase-based iris recognition algorithm dedicated to compact hardware implementation. Fig.2(a) shows the baseline algorithm for iris recognition, which consists of a preprocessing stage and a matching stage. Here we briefly overview these stages.

A. Preprocessing

An iris image contains some irrelevant parts (e.g., eyelid, sclera, pupil, etc.). Also, the size of an iris may vary depending on camera-to-eye distance and lighting condition. Therefore, the original image needs to be normalized.

1. Iris Localization

This step is to detect the inner (iris/pupil) boundary and the outer (iris/sclera) boundary in the original image. We model the inner boundary as an ellipse, and the outer boundary as a circle.

2. Iris Normalization

Next step is to normalize iris images to compensate for iris deformation. In order to avoid eyelashes, we use only lower half portion of the iris (Fig.2(b)) and unwrap the region to a rectangular block of a fixed size (128×256 pixels) as illustrated in Fig.2(c). The eyelid region is then masked as in Fig.2(d).

B. Matching

The key idea of the proposed algorithm is to use phase-based image matching for image alignment and matching score calculation (see Fig.2 (a)). Before discussing the algorithm, we introduce the principle of phase-based image matching using the Phase-Only Correlation (POC) function. Consider two $N_1 \times N_2$-pixel images, f (n_1, n_2) and g (n_1, n_2), where we assume that the index ranges are $n_1 = -M_1, \cdots, M_1$ ($M_1 > 0$) and $n_2 = -M_2, \cdots, M_2$ ($M_2 > 0$) for mathematical simplicity, and hence $N_1 = 2M_1+1$ and $N_2 = 2M_2+1$. Let F (k_1, k_2) and G(k_1, k_2) denote the 2D DFTs of the two images. The cross-phase spectrum RFG (k_1, k_2) is given by

$$R_{FG}(k_1,k_2)=\frac{F(k_1,k_2)\overline{G(k_1,k_2)}}{|F(k_1,k_2)\overline{G(k_1,k_2)}|}=e^{j\theta(k_1,k_2)}, \quad (1)$$

where $k_1 = -M_1, \cdots, M_1$, $k_2 = -M_2, \cdots, M_2$, $\overline{G(k_1, k_2)}$ is the complex conjugate of $G(k_1, k_2)$ and $\theta(k_1, k_2)$ denotes the phase difference of $F(k_1, k_2)$ and $G(k_1, k_2)$. The POC function $r_{fg}(n_1, n_2)$ is the 2D Inverse DFT of $RFG(k_1, k_2)$. When two images are similar, their POC function gives a distinct sharp peak. When they are not similar, the peak drops significantly. The height of the peak gives a good similarity measure for image matching, and the location of the peak shows the translational displacement between the images. Our

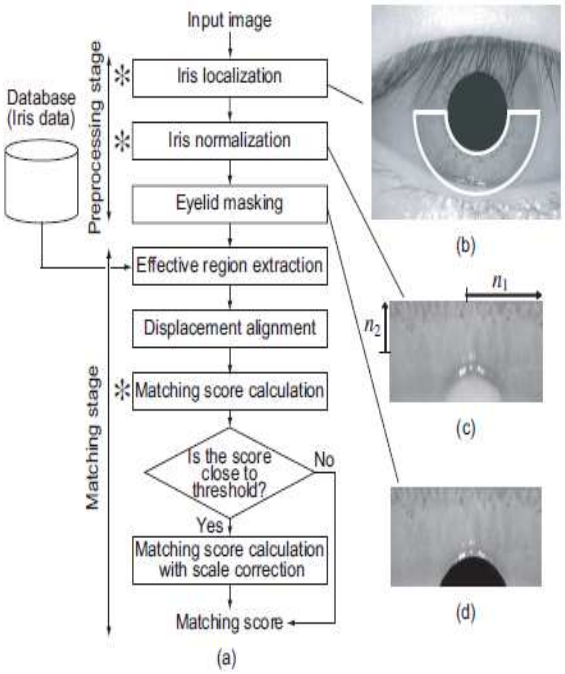

Fig.2. Baseline algorithm: (a) flow diagram, (b) original image, (c) normalized image (n_1 axis corresponds to the angle of polar coordinate system and n_2 axis corresponds to the radius), and (d) normalized image with eyelid masking.

observation shows that the 2D DFT of a normalized iris image contains meaningless phase components in high frequency domain, and that the effective frequency band of the normalized iris image is wider in k_1 direction than in k_2 direction(see Fig.3). To evaluate the similarity using the inherent frequency band within iris textures, we employ BLPOC (Band-Limited Phase-Only Correlation) function. Assume that the ranges of the significant frequency band are $k_1 = -K_1, \cdots, K_1$ ($0 \le K_1 \le M_1$) and $k_2 = -K_2, \cdots, K_2$ ($0 \le K_2 \le M_2$), where as shown in Fig. 3(b). Thus, the effective size of frequency spectrum is given by $L_1 = 2K_1+1$ and $L_2 = 2K_2+1$. The BLPOC function is given by

$$r_{fg}^{K_1K_2}(n_1,n_2)=\frac{1}{L_1L_2}\sum_{k_1,k_2}R_{FG}(k_1,k_2)W_{L_1}^{-k_1n_1}W_{L_2}^{-k_2n_2}, \quad (2)$$

Where, $n_1 = -K_1, \cdots, K_1$, $n_2 = -K_2, \cdots, K_2$, $W_{L1} = e^{-j\frac{2\pi}{L_1}}$, $W_{L2} = e^{-j\frac{2\pi}{L_2}}$ and $\Sigma_{k1,k2}$ denotes $\sum_{k_1=-K_1}^{K_1}\sum_{k_2=-K_2}^{K_2}$. Fig.4 shows an example of genuine matching using the original POC function and the BLPOC function. The BLPOC function provides better discrimination capability than that of the original POC function. In the following, we describe the detailed process of the matching stage(shown in Fig.2(a)) using the BLPOC function.

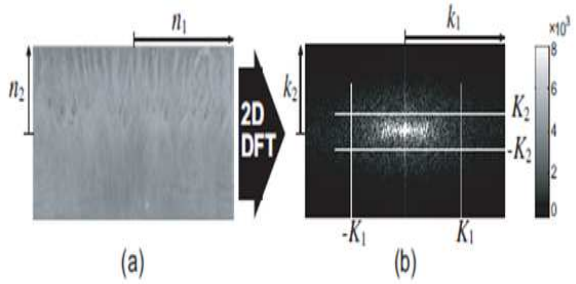

Fig.3. Normalized iris image in (a) spatial domain, and in (b) frequency domain (amplitude spectrum), where $K_1 = 0.55M_1$ and $K_2 = 0.2M_2$.

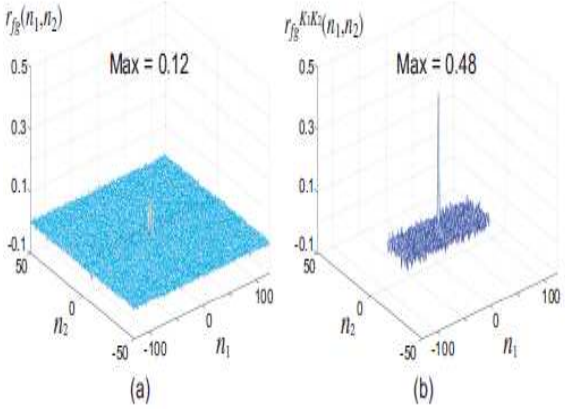

Fig.4. Example of genuine matching using the original POC function and the BLPOC function: (a) original POC function r_{fg} (n_1, n_2), and (b) BLPOC function $r_{fg}^{K_1 K_2}(n_1, n_2)$.

1. Effective region extraction: Given a pair of normalized iris images ˜ $f(n_1, n_2)$ and ˜$g(n_1, n_2)$ to be compared, the purpose of this process is to extract the effective regions $f(n_1, n_2)$ and g(n1, n2) of the same size as illustrated in Fig.5(a). When the extracted region becomes too small to perform image matching, we extract multiple effective sub-regions from each iris image by changing the width parameter w (Fig.5(b)). In our experiments, we extract 6 sub-regions from an iris image by changing the parameter w as 55, 75 and 95 pixels.

2. Displacement alignment: This step is to align the translational displacement between the extracted regions. The displacement parameters can be obtained from the peak location of the BLPOC function $r_{fg}^{K_1 K_2}(n_1, n_2)$.

3. Matching score calculation: We calculate the BLPOC function between the aligned images and evaluate the matching score as the maximum correlation peak value. When multiple sub-regions are extracted as illustrated in Fig.5(b), the matching score is calculated by taking an average for effective sub-regions. If the matching score is close to threshold value to separate genuine and impostors, we calculate the matching score with scale correction.

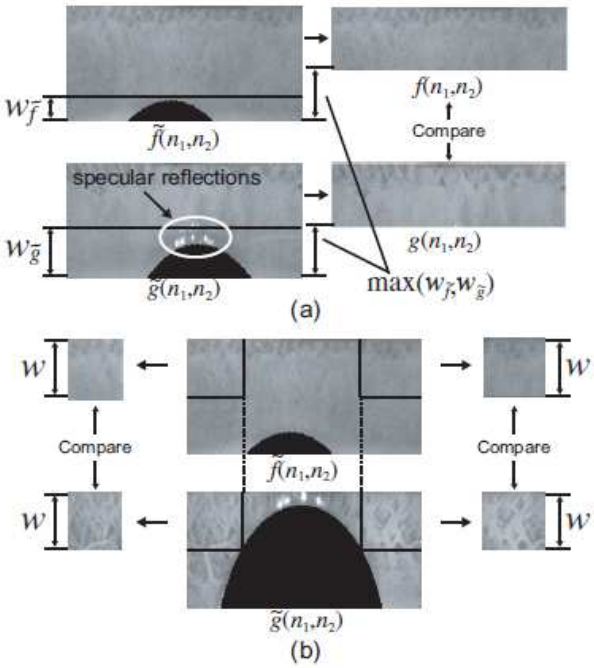

Fig.5. Effective region extraction: (a) normal case, and (b) case when multiple sub-regions should be extracted.

C. Simplified Algorithm

For typical embedded systems, the overall iris recognition algorithm should be implemented within a single DSP or an MPU (Micro Processing Unit), which imposes severe limitations on available computation power. Hence, we consider here a simplified version of the original algorithm, where only the marked "*" three steps in Fig.2(a) are adopted, while omitting other four steps. An important advantage of the simplified algorithm is that we do not need to register the iris "image" data directly in the system. In practice, only the Fourier phase components are to be stored in the system.

III. IRIS RECOGNITION SYSTEM

We have already developed commercial fingerprint verification units using phase-based image matching. The goal of this paper is to demonstrate that the same approach is also effective for designing iris recognition devices. Note that conventional iris recognition devices are large and expensive in general. We can implement a compact DSP-based iris recognition system using the simplified algorithm described in the previous section. Fig.6 (a) shows the developed iris recognition device of size 15cm×10cm×3.5cm (HWD).

A. System Architecture

Fig.6(b) shows the block diagram of the device, which consists of two PWBs (Printed Wiring Boards), camera PWB and DSP PWB. The camera PWB contains a pair of cameras with surrounding infrared

LEDs for lighting, and a full-color LED for status indication. Camera resolution is 1320×1024 pixels and only 640×480 pixels fixed area is used for image processing. An infrared band-pass filter is attached to each camera to capture infrared iris images. The DSP PWB contains a DSP, a Flash ROM, two dynamic and one static RAM chips, a codec for voice message, and a serial communication port. The DSP is well suited for 2D DFT computation required for phase-based image matching. In our system, a fixed-point DSP is used because it runs at higher clock frequency with lower power consumption compared with floating-point DSPs.

B. Procedure of Iris Recognition

For capturing good-quality iris images, the device has mechanisms of a rotatable camera head, a mirror for face positioning, and an LED status indicator. The status LED changes its color depending on camera-to-eye distance. Fig.7(a) shows the operation flowchart for the iris recognition device, which consists of (i) the image capture stage and (ii) the iris recognition stage. We adopt the simplified algorithm described in the Section C of II for the iris recognition stage.

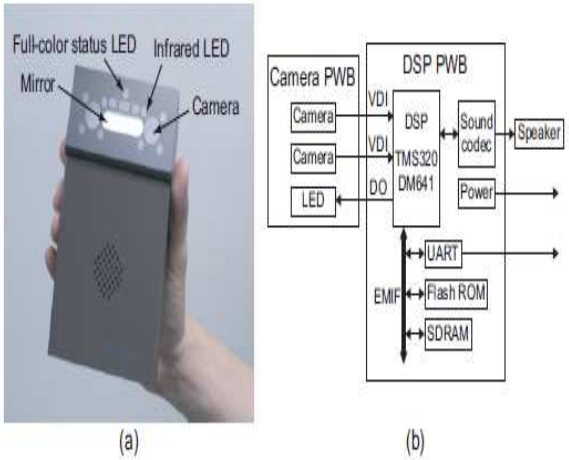

Fig.6. Iris recognition system: (a) prototype of the device, and (b) block diagram.

The purpose of the image capture stage, on the other hand, is to capture iris images at the specified distance (~10cm in our prototype system). To do this, the system estimates the camera-to-eye distance from corneal reflection patterns of infrared LEDs. Fig.7(b) shows an example of captured iris image, where corneal reflections of four infrared LEDs are observed. First, the system detects the four-point reflections by using a 41×41 spatial filter shown in Fig.7(c). The filtered image is shown in Fig.7(d). If there exists a clear four-point reflection pattern, the filter outputs a sharp peak at the center of the pattern. After detecting the four-point pattern, the system can estimate the camera-to-eye distance using the size of the pattern. Only when the size is in an appropriate range, the captured image is used for recognition. In our prototype, the overall iris recognition procedure (Fig.7(a)) takes only 1 second on the state-of-the-art DSP (Texas Instruments TMS320 DM641 400MHz), which clearly demonstrates a potential possibility of DSP-based iris recognition applicable to a wide range of embedded applications.

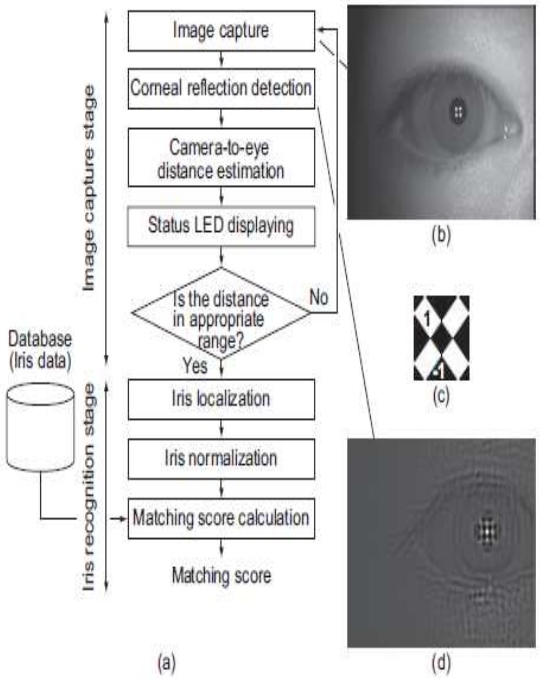

Fig.7. Procedure of iris recognition: (a) overall procedures, (b) example of captured iris image, (c) filter for reflection detection, and (d) filtered image.

IV. EXPERIMENTS AND DISCUSSIONS

This section describes a set of experiments using the CASIA iris image database ver. 1.0 and ver. 2.0 for evaluating matching performance.

1. CASIA iris image database ver. 1.0: This database contains 756 eye images with 108 unique eyes and 7 different images of each unique eye. We first evaluate the genuine matching scores for all the possible combinations of genuine attempts; the number of attempts is 7C2×108=2268. Next, we evaluate the impostor matching scores for all the possible combinations of impostor attempts; the number of attempts is 108C2×72=283122.

2. CASIA iris image database ver. 2.0: This database contains 1200 eye images with 60 unique eyes and 20 different images of each unique eye. We first evaluate the genuine matching scores for all the possible combinations of genuine attempts; the number of attempts is 20C2×60=11400. Next, we evaluate the impostor matching scores for 60C2×42=28320 impostor attempts, where we take 4 images for each eye

and make all the possible combinations of impostor attempts.

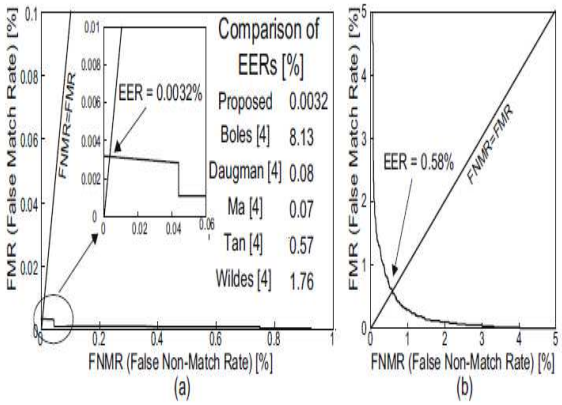

Fig.8. ROC curve and EER: (a) CASIA iris image database ver. 1.0, and (b) ver. 2.0

Fig.8(a) shows the ROC(Receiver Operating Characteristic) curve of the proposed algorithm for the database ver.1.0. The ROC curve illustrates FNMR (False Non-Match Rate) against FMR (False Match Rate) at different thresholds on the matching score. EER(Equal Error Rate) shown in the figure indicates the error rate where FNMR and FMR are equal. As is observed in the figure, the proposed algorithm exhibits very low EER(0.0032%). Some reported values of EER from [5] using the CASIA iris image database ver. 1.0 is shown in the same figure for reference. Note that the experimental condition in [5] is not the same as our case, because the complete database used in [5] is not available at CASIA due to the limitations on usage rights of the iris images. Fig.8 (b) shows the ROC curve for the database ver. 2.0. The quality of the iris images in this database are poor and it seems that the recognition task is difficult for most of the reported algorithms. Although we cannot find any reliable official report on recognition test for this database, we believe that our result(EER=0.58%) may be one of the best performance records that can be achieved at present for this kind of low-quality iris images. All in all, the above mentioned two experimental trials clearly demonstrate a potential possibility of phase-based image matching for creating an efficient iris recognition system.

V. CONCLUSIONS

The authors have already developed commercial fingerprint verification units using phase-based image matching. In this paper, we have demonstrated that the same approach is also highly effective for iris recognition task. It can also be suggested that the proposed approach will be highly useful for multimodal biometric system having iris and fingerprint recognition capabilities.

VI. REFERENCES

[1] Kazuyuki Miyazawa, Koichi Ito, Takafumi Aoki, Koji Kobayashi, and Hiroshi Nakajima, "A Phase-Based Iris Recognition Algorithm", Proc. Vision Interface (2006) 394–399.

[2] Wayman, J., Jain, A., Maltoni, D., Maio, D.: Biometric Systems. Springer (2005).

[3] Jain, A., Bolle, R., Pankanti, S.: Biometrics: Personal Identification in a Networked Society. Norwell, MA: Kluwer (1999).

[4] Daugman, J.: High confidence visual recognition of persons by a test of statistical independence. IEEE Trans. Pattern Analy. Machine Intell. 15 (1993) 1148–1161.

[5] Ma, L., Tan, T., Wang, Y., Zhang, D.: Efficient iris recognition by characterizing key local variations. IEEE Trans. Image Processing 13 (2004) 739–750.

[6] Boles, W., Boashash, B.: A human identification technique using images of the iris and wavelet transform. IEEE Trans. Signal Processing 46 (1998) 1185–1188.

[7] Tisse, C., Martin, L., Torres, L., Robert, M.: Person identification technique using human iris recognition. Proc. Vision Interface (2002) 294–299.

[8] Wildes, R.: Iris recognition: An emerging biometric technology. Proc. IEEE 85 (1997) 1348–1363.

[9] Kumar, B., Xie, C., Thornton, J.: Iris verification using correlation filters. Proc. 4th Int. Conf. Audio- and Video-based Biometric Person Authentication (2003) 697–705.

[10] Kuglin, C.D., Hines, D.C.: The phase correlation image alignment method. Proc. Int. Conf. on Cybernetics and Society (1975) 163–165.

[11] Takita, K., Aoki, T., Sasaki, Y., Higuchi, T., Kobayashi, K.: High-accuracy sub pixel image registration based on phase-only correlation. IEICE Trans. Fundamentals E86-A (2003) 1925–1934.

[12] Takita, K., Muquit, M.A., Aoki, T., Higuchi, T.: A sub-pixel correspondence search technique for computer vision applications. IEICE Trans. Fundamentals E87-A (2004) 1913–1923.